EARTH OBSERVATION AND GEOMATICS ENGINEERING
website: https://eoge.ut.ac.ir

Automatic change detection in remotely sensed hyperspectral imagery (Case study: wetlands and waterbodies)

Mahdi Hasanlou*, Seyd Teymoor Seydi

School of Surveying and Geospatial Engineering, College of Engineering, University of Tehran, Tehran, Iran

Article history:
Received: 24 July 2017, Received in revised form: 1 February 2018, Accepted: 14 March 2018

ABSTRACT

Wetlands are one of the important types of ecosystems that play a fundamental role in the environment and provide significant benefits due to the resources that they contain. Therefore, it is necessary to monitor the changes in these ecosystems. The alterations in Earth's ecosystems caused by the natural activities, such as drought, as well as human activities and population growth has been affecting the wetlands and waterbodies area. Therefore, for achieving a better detection of these changes over time, it is important to generate descriptive location maps based on the characteristics of wetlands. Hyperspectral images have shown potential use in many applications due to their high spectral resolution, and consequently, their high informative value. This study presents a hybrid procedure for automatic detection of changes in wetlands using a new approach which can provide more details about the changes with high accuracy. The hybrid proposed method is based on incorporating chronochrome, Z-score analysis, Otsu algorithm, simplex via split augmented lagrangian (SISAL), Harsanyi–Farrand–Chang (HFC), Pearson correlation coefficient (PCC), and support vector machine (SVM) to detect changes using hyperspectral imagery. The proposed method in the first step, produce a training data for tuning SVM and kernel parameters. The second step, predicted change areas based on a chronochrome algorithm and binary change map obtained using SVM classifier. The third step, the amplitude of changes is created by Z-Score analysis and binary change mask. Finally, the multiple change map is produced based on the estimation of number and extraction of endmembers and similarity measure. The proposed method evaluated and compared the performances with other common hyperspectral change detection methods using three real-world datasets of multi-temporal hyperspectral imagery. The empirical results reveal the superiority of the proposed hybrid method in extracting the change map with an overall accuracy of nearly 96% and a kappa coefficient of 0.89 while other hyperspectral change detection methods have the overall accuracy lower than 93% and kappa coefficient 0.80. In addition, this hybrid method can provide 'multiple changes' as well as the magnitude of extracted changes.

KEYWORDS

Change detection
Hyperspectral
Wetlands
Multiple-change

1. Introduction

Wetlands are one of the most influential ecosystems in the natural environment for which it is very difficult to find an alternative (White et al.,2015). There are many definitions of wetlands. The U.S. Army Corps of Engineers defined wetlands as "Those areas that are inundated or saturated by surface or groundwater at a frequency and duration sufficient to support, and that under normal circumstances do support, a prevalence of vegetation typically adapted for life in saturated soil conditions". Wetlands cover nearby %6-%7 of Earth surface (Keramitsoglou et al., 2015; Mereta et al., 2012) and provide many vital benefits for the environment such as: improving the quality of water, controlling the soil erosion, recharging underground water tables, sustaining

* Corresponding author
E-mail addresses: hasanlou@ut.ac.ir (M. Hasanlou); seydi.teymoor@ut.ac.ir (S.T. Seydi)
DOI: 10.22059/eoge.2018.238510.1010

against flooding, filtering toxic material and sediments, providing a defense mechanism against sandstorms, and providing food and habitat for wildlife (Jiang et al.,2014; Romshoo & Rashid, 2014; Whiteside & Bartolo, 2015).

The earth's ecosystems are continuously changing due to human activities and natural phenomena (Gibbes, et al., 2009). Such changes on wetlands are usually caused by reasons such as dry seasons, alterations in groundwater, and habitat heterogeneity (Rapinel et al., 2015; Romshoo & Rashid, 2014; Taminskasa, Petro\liusa et al., 2013). Remote sensing is a tool that can play a very beneficial role in monitoring and studying of the changes in the environment, especially in wetlands, on local and global scales (Mabwoga & Thukral, 2014; McCarthy et al., 2015). In fact, remote sensing can provide data from the environment in large scale and real-time with minimum cost and time-consumption (Bovolo & Bruzzone, 2015; Gomez, 2001). These properties have made remote sensing a very effective approach in the fields of earth and environment sciences, especially in change detection applications (Hasanlou & Seydi, 2018; Huang et al., 2017; S. Liu, 2015a; Storey et al., 2017).

Change detection is a process that aims to measure the difference between two objects at different times (Li et al., 2011; Lu et al., 2011; Singh, 1989). One benefit of change detection is to help manage a system more efficiently by using temporal data (Thonfeld et al., 2016). Also, detection of changes can help us create accurate change models based on the past information to avoid disastrous events (Hegazy & Kaloop, 2015; Thonfeld et al., 2016). With the development of remote sensing systems, it is possible to obtain data from objects in the high spectral resolution which is known as hyperspectral imagery (George et al., 2014). The high spectral resolution of the data helps with distinguishing objects that seem very similar (Barrett, 2013; S. T. Seydi & Hasanlou, 2018; Smith, 2012; Yuen & Richardson, 2010).

During the recent years, the most relevant studies on change detection in wetlands have been using remote sensing data. Sica et al. (2016a) study on Paraná River Delta located in Argentina, where change analysis was performed based on post-classification via the supervised method and SVM classifier. Also, Seydi & Hasanlou (2016a) studied the Shadegan wetlands located in Iran. This research proposed a new hybrid method for detecting changes which used a semi-supervised method based on iteratively reweighted multivariate alteration detection (IR-MAD) algorithms, Z-score analysis, and Otsu algorithm. They also used hyperspectral image data-sets. In an older study, Ghobadi et al. (2015) studied the Al Hawizeh wetlands located in the southwest region of Iran. For change analysis, they used maximum likelihood as the post-classification methods and classifier on the Landsat datasets (OLI, MSS, and ETM).

Mousazadeh et al. (2015) studied Anzali wetlands in Iran, where their approach integrated supervised classification using maximum likelihood classifier, and zonal and object-oriented image analyses. Also, in their study, Landsat-8 and digital topographic maps dataset were used. In another work, Yang & Yan (2016) conducted a change analysis study on Poyang Lake wetland in China where they used supervised classification procedures using error correcting output code (ECOC) and SVM algorithm. Also in their study, the hydrological data and remotely sensed data contained: TM, ETM, OLI, and TIRS. Gunawardena et al. (2014) monitored the eastern river basin region in Sri Lanka using supervised classification methods and Landsat datasets including ETM+, ALOS-AVNIR2, and ALOS-PALSAR images.

Zanotta et al. (2013) studied central portion of South American areas, specifically the Brazilian Pantanal. In their work, they proposed automatic hybrid methods based on expectation maximization (EM), Bayes theorem, and image difference detection. Also, their method showed improvements in change detection efficiency by incorporating morphology operators using Landsat dataset for change analysis. Kayastha et al. (2012) analyzed an area in northern Virginia for change detection using Z-score and the tasseled cap algorithm. In their paper, threshold selection was performed based on time series analysis of Landsat ETM data-sets.

Wu et al. (2012a) studied the Poyang Lake in China for change analysis using supervised methods based on adaptive coherence/cosine estimator (ACE) detector on stacks of hyperspectral datasets. In another study, Dronova et al. (2011) measured the duration of the low water period at Poyang Lake in China for change analysis. They incorporated supervised post-classification methods based on a fuzzy method to perform a semi-automated selection of training objects on Landsat TM dataset. Also, Lee (2011) studied the wetlands in western Canada to extract the change map by using post-classification (maximum likelihood classifier) on multi-temporal Landsat-7 data-sets. Furthermore, Zhao et al. (2010a) analyzed the change map on Pearl River estuary, which is located in China, by using a post-classification method (decision tree classifier) on the Landsat MSS, ETM+ and TM dataset.

By considering both the change detection methods and the employed data-sets in related literature, it can be observed that there are several challenges in change detection on wetland regions. First, we can see that the most frequently used procedure for change detection is the post-classification method. Secondly, most wildly used image datasets for application of change detection in wetland areas are different types of Landsat imagery. Therefore, there is a lack of research based on hyperspectral images for change detection applications. On the other hands, hyperspectral imagery has displayed high potential for many applications such as classification and change detection. Also, several studies have been conducted about this type of imagery (Hasanlou et al., 2015; Kumar & Sinha, 2014) which can be considered to be applied in monitoring changes in the wetlands and

waterbodies areas.

The change detection methods using remote sensing imagery can be divided into five groups. The first group includes post-classification comparison-based procedures (Castellana et al., 2007). In this group, the post-classification comparisons are widely used for detecting changes based on comparing classified images in a pixel by pixel class label manner (Dronova et al., 2011; Lee, 2011; Zhao et al., 2010b). This group provides 'multiple-change' or 'from-to' information and is not affected by the atmospheric conditions and sensor differences in the acquisitions data. However, prior knowledge for training set is necessary for this group, which is a big challenge for supervised methods due to the fact that acquiring training sets in multi-temporal data sets can be very difficult (S. Liu, 2015a; Shah-Hosseini, et al., 2015a). When using hyperspectral imagery, it is inevitable to use dimension reduction procedures due to Hughes phenomenon (Samadzadegan et al., 2012). Also, for unsupervised methods, it is necessary to label the classes to be able to analyze the change map (Shah-Hosseini et al., 2015a). The accuracies of both supervised and unsupervised change detection methods depend on the performance of the utilized classifier algorithm (S. Liu, 2015a; Shah-Hosseini et al., 2015a). The common supervised post-classification comparison-based methods are maximum likelihood (ML) (Lee, 2011; Mousazadeh et al., 2015; Yang & Yan, 2016), SVM (Sica et al., 2016b; Yang & Yan, 2016), and Random Forest (RF) classifiers (Franklin et al., 2015). Also, the common unsupervised methods are ISODATA classifier (Omo-Irabor, 2016), Fuzzy C-means (FCM) (Ghosh et al., 2011), and K-means (KM) (Fröjse, 2011). The second group of change detection methods that use hyperspectral imagery uses direct multi-date classification (DMC) based on using one classifier algorithm on stacks of multi-date data-sets (Ahlqvist, 2008). In this group, due to the utilization of one classifier, the computational cost of classification is low. However, this group of methods suffers from drawbacks such as providing little knowledge about the 'from-to' information, and the fact that for supervised methods it is necessary to have training-sets (Shah-Hosseini et al., 2015b; Yuan et al., 2005). The third group of methods includes similarity-based methods where the spectral signature of objects is measured (Adar et al., 2012). Advantages of these methods include the simplicity of implementing them and their low computational cost. Nevertheless, they can be affected by noise and atmospheric conditions (S. Liu, 2015b; Shah-Hosseini et al., 2015b). The fourth group is the transformation-based methods where the dataset is transformed from image space to feature space (Pieper et al., 2015; Shah-Hosseini et al., 2015b; K. M. Vongsy, 2007a). These methods have high potential in processing data with high dimensionality, and thus, high capability in change detection. The common transformation-based methods including principal component analysis (PCA) (K. Vongsy et al., 2009), multivariate alternative detection (MAD) (Nielsena & Müllerb, 2003a), Chronochrome (CC) (Michael et al., 2008a), and cross equalization (CE) (Michael T. Eismann et al., 2008a). The fifth group is hybrid based procedures that combine couples of previous methods in order to achieve new automatic or unsupervised methods (Bovolo et al., 2012; Shah-Hosseini et al., 2015b).

We described five change detection groups and briefly investigated their pros and cons. Generally, there are many challenges in hyperspectral change detection (HCD) including (1) the outputs of many segment-based threshold selection procedures are not perfect, therefore these methods require clear histograms of change and no-change areas. Also, some change detection methods require hyper-parameter tuning, which is necessary to be performed based on experimental knowledge (Shah-Hosseini et al., 2015c), (2) Many of the automatic methods do not provide information about of nature of changes, and only provide the binary change maps, while multiple change information is important for decision making. Moreover, these methods do not provide the amplitude of changes (Hussain et al., 2013a; Shah-Hosseini et al., 2015c). Also, some of change detection methods need to knowledge-based threshold that it is hard to set. (3) However, the post-classification and direct-classification methods could be provided a multiple-change map or 'from-to' information but these methods are supervised, therefore providing training data is inevitable. However, collection of this training data can be very difficult and (4) as described in the literature review in the previous section, many of the studies used multispectral dataset to monitor the wetland regions, therefore, there is a lack of research that investigates the capabilities of hyperspectral imagery in change detection in wetlands and waterbody areas. Nevertheless, the series of spaceborne sensors (e.g., EnMAP, PRISMA, and HyspIRI) will be launched on a schedule that will increase the availability of hyperspectral imagery with improvement in data quality. With this regards, it is necessary to utilize data-sets that provide more detail about changes.

Wetlands are very sensitive ecosystems, which implies that monitoring of their changes is necessary for protecting them. In order to provide a monitoring framework to address this issue, we need to focus on informative image data-sets and accurate methods. The change detection problem could be solved in a simple framework. There are many novel algorithms proposed by researchers for detection of changes using of hyperspectral imagery that solved change detection in a complex framework. Therefore, these novel methods improve performance change detection but the change detection problems become more complex and hard. So, this research proposed a change detection method for hyperspectral imagery on wetland and waterbody areas using conventional algorithms. The main novelty proposed method is simple theme nonetheless preserved accuracy. Addition,

the proposed method could be applied in an automatic framework and provides more details of nature of changes. The main purpose of this paper is to propose a change detection hybrid method that addresses the previously mentioned change detection issues. In addition, this study has a number of minor objectives including (1) sensitivity assessment of different kernel functions on hybrid change detection (HCD) (2) evaluating the effects of normalization steps on input data on the performance of the SVM classifier. In fact, the proposed method is a new hybrid change detection (HCD) method based on Otsu algorithm, CC, Z-score, PCC, and SVM, and has three phases including (1) global predictor phase, (2) analysis phase, and (3) decision phase. More specifically, the global predictor uses CC algorithm for highlighting change and no-change area, the phases analysis uses the SISAL, HFC and Z-score analysis for data analysis, and in the decision phase the SVM classifier, Otsu algorithm, and PCC are used to obtain the binary change map, amplitude of change map, and the 'multiple-change' information map. The criteria selection mentioned methods in proposed framework are simple for implementation and robust for the analysis of high dimensional. Addition, the source codes these methods are available. This hybrid method benefits from several advantages that distinguish it from other change detection methods including: (1) sensitivity to subtle changes with high accuracy and low false alarms rates, (2) providing the 'multiple-change' information and amplitudes of changes in addition to binary change map (3) simple implementation compared to common HCD methods, (4) low computational cost and the ability to process high-dimensional data, (5) no need for training set or its unsupervised framework and (6) incorporating hyperspectral datasets which have high potentials in most applications specially for change detection analysis. The rest of this paper is organized as follows: section 2 describes the general proposed methodology. The details of the proposed method are presented in section 3, and section 4 presents the experimental results of this method.

2. Proposed Hybrid Method

From the output point of view, each pixel in the multi-temporal dataset has two states: change or no-change state. The flowchart of the proposed method is illustrated in Figure 1. The proposed hybrid method has three different outputs: the first output is a binary change map, the second output is the amplitude of changes, and finally, the third output is the multiple change map. The next subsection explains these outputs in more detail.

2.1 Global predictor phase

The main purpose of the predictor phase is to distinguish the change area from the no-change area. For this purpose, CC algorithm was used to transfer the data from the image space to the feature space. The output of this phase is a cubic form data with dimensions equal to the dimensions of the input hyperspectral datasets.

2.2 Analysis phase

The analysis phase is applied for two purposes, (1) extraction and estimation of endmembers on masked stack data which is performed using HFC and SISAL algorithms, and (2) the output of the CC method is cubic data, therefore to aggregate and standardize the output of CC method, the Z-score analysis was applied, and then the single band data was generated. After extracting and estimating the endmembers,

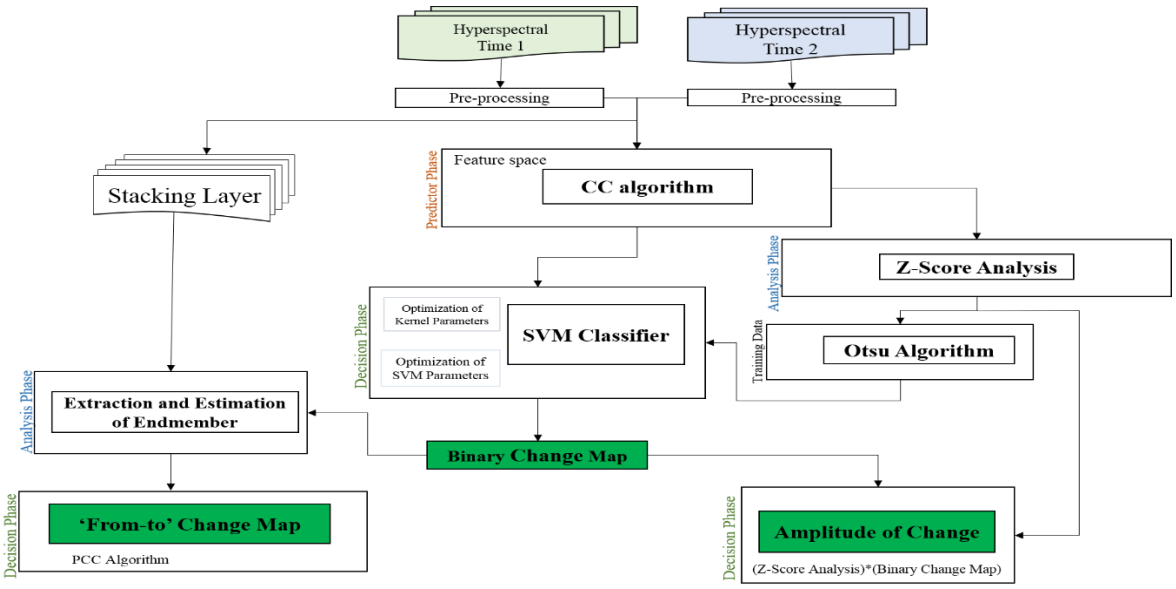

Figure 1. An overview of the proposed method and three blue output boxes

the PCC method is applied to generate the 'multiple-change' map. The output of Z-score analysis is used for two purposes: (1) the Z-score analysis is used in combination with the Otsu algorithm in order to generate unsupervised training data, and (2) this method combines binary change maps for extracting the amplitude of change map as single output.

2.3 Decision phase

The decision phase is used for (1) locating the change and no-change pixels (i.e. binary change map), (2) extracting 'multiple-change' information, (3) calculating the amplitude of the change map, and (4) automatically generating training data. This phase uses three algorithms: the SVM classifier, the Otsu algorithm, and the PCC algorithm.

2.3.1 Training data generation

This part explains the automatic production of training data for SVM classifier by incorporating the Otsu algorithm over the output of CC and the Z-Score analysis. After pre-processing of input multi-temporal hyperspectral datasets, the first step in the flowchart of the proposed method begins with applying CC transformation and the transfer of data from the image space to the feature space. The second step of the proposed method is to implement the Otsu algorithm for producing the initial change map. This initial change map contains several change pixels mixed with no-changed pixel (i.e. unfavorable change pixels) (Figure 2). Therefore, for the initial change map that contains two classes, change, and no-change, the Otsu algorithm is applied once again for each of the previous output classes on the Z-score pixels and the three classes are divided according to Figure 1.

This process causes more isolation and increases the reliability of change and no-change pixels. The main reason for dividing the three classes is that the first class for no-change class and third class for change contain many noise pixels because the noise has the minimum value and the maximum value. Therefore, the first class for no-change and the third class for change are eliminated. The third class for no-change and first class for change contain mixed pixels of change with no-change, therefore these classes are also removed. In the next step, the pixels whose locations are found via the output of the CC algorithm are selected as the training set for the SVM classifier.

2.3.2 Tuning SVM's Kernel Parameters

After producing training data, the parameters of the SVM classifier, including the optimal kernel parameters, are tuned. In this regard, the prepared input datasets are divided into two groups: (1) training data (30% of pixels) and (2) testing data (70% of pixels). The tuning parameters are based on grid search (GS) and evaluation type is cross-validation that a range is defined for the parameters of kernel and SVM. The SVM classifier is trained using training data based on the defined value of in GS then model made evaluated on training data used criteria such as overall accuracy. The process repeated until are covered all of the range. Finally, the best value of accuracy is equal to tune parameters.

2.3.3 Binary Change Map

In the next step, the SVM classifier (based on obtained tune parameters in the previous section) is applied to the output of the CC algorithm. The output of this classifier is a binary change map (i.e. a map with two classes: change and no-change pixels). The binary change map is determined by assigning each pixel in the image space change or no-change values. The values of change pixels are set to one, and the no-change pixels are set to zero.

2.3.4 Amplitude of Change

The amplitude of change map shows the intensity of change. Thus, a high-intensity value represents higher change. The amplitude of change map is extracted by multiplying the final binary change map by Z-Score values, as shown in Figure 3.

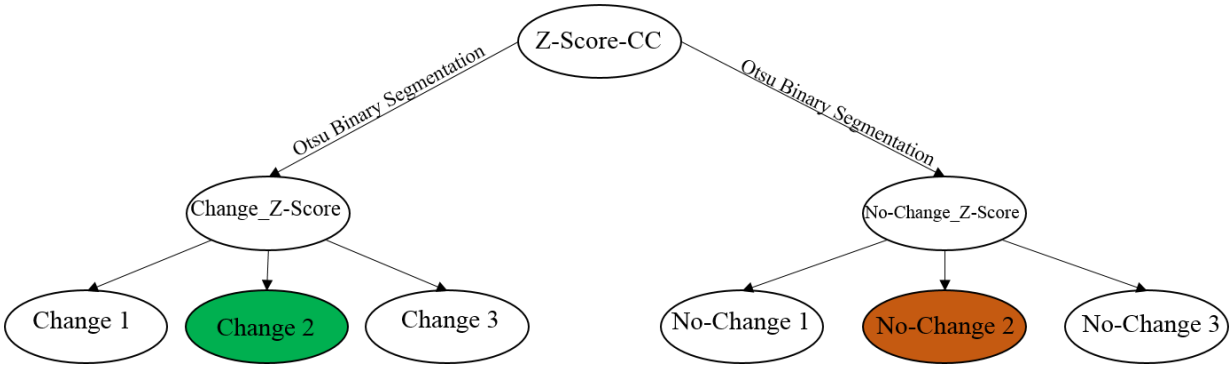

Figure 2. Extraction of training data using of iterative Otsu algorithm

3.5 Extracting 'Multiple-change' Information

Retrieving accurate 'multiple-change' change information is required in many change detection analysis (Hussain et al., 2013b). In this study, 'multiple-change' information is created based on estimation and extraction of endmembers in the multi-temporal hyperspectral dataset. For this purpose, these four steps are required: (1) masking the change area on stack hyperspectral dataset using final binary change map, (2) estimating endmembers by using HFC methods, (3) extracting endmember using SISAL algorithm, and (4) assigning a label for each pixel by finding maximum similarity between pixels of stacking layers and the extracted endmembers by incorporating PCC algorithm. To produce the 'multiple-change' map, it is necessary to assign a label to each endmember. Therefore, the PCC algorithm measures the similarity between each endmember and each pixel in stacked hyperspectral data. Usually, assigned labels correspond to endmembers with the highest similarity value. In next step, pixels with high similarity values related to one of the endmembers are assigned their corresponding labels (Figure 4).

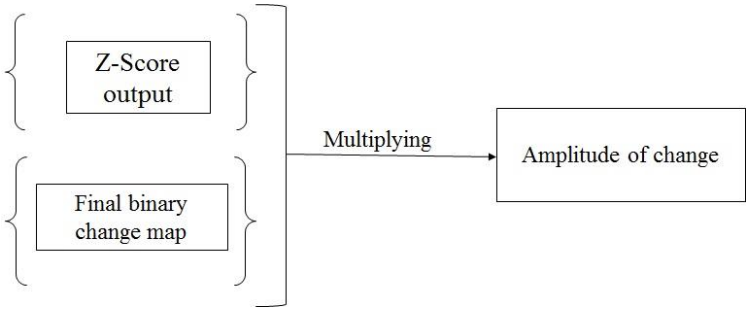

Figure 3. The flowchart of computing amplitude of change

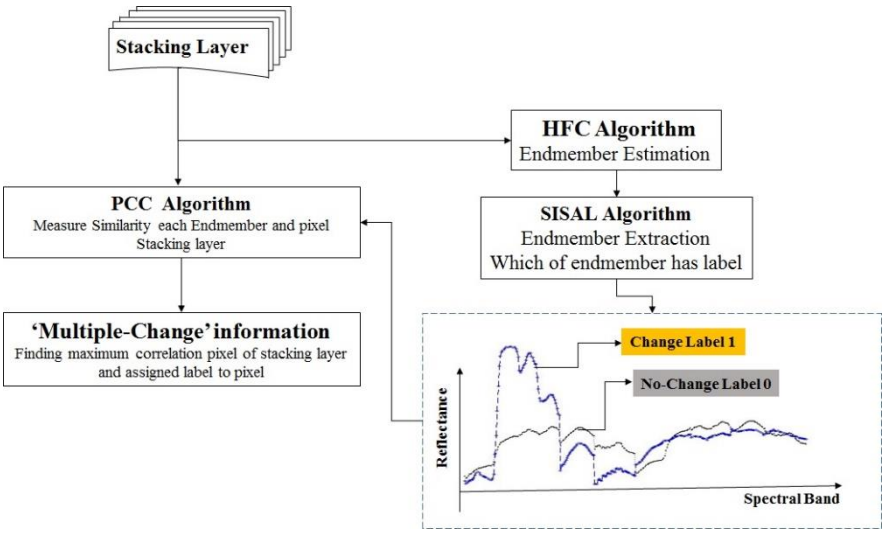

Figure 4. The flowchart retrieving 'multiple-change' information

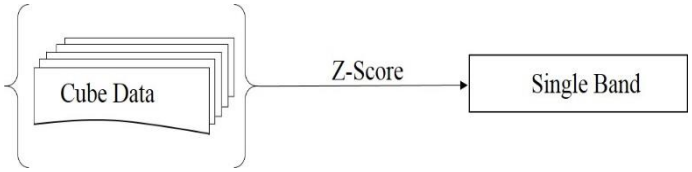

Figure 5. The output of Z-score analysis has single band

3. Methodology

As discussed in the previous section, proposed hybrid method consists of six main algorithms (Figure 1), (1) chronochrome (CC), (2) Z-score analysis, (3) Otsu algorithm, (4) the SVM classifier, (5) endmember extraction and estimation algorithm, and (6) Pearson correlation coefficient (PCC). Also, the proposed method consists of three main phases including (a) predictor phase, (b) analysis phase, and (c) decision phase. These algorithms and phases are described in more detail in this section.

3.1 Chronochrome

The Chronochrome approach, proposed by Stocker and Schaum, provides a prediction based on the joint second-order statistics between the reference and test images (Michael T. Eismann et al., 2008a; Schaum & Stocker, 1998). The main purpose of this method is to estimate the background in the test image as a linear function of the reference image and detect the changes on the resulting difference image (Schaum & Stocker, 1998; K. M. Vongsy, 2007a). For this purpose, given *x*, a linear predictor is fitted for *y*. The centered covariance and cross-covariance is computed before fitting a linear estimation to *y*-data as a function of the *x*-data (Eq. (1)).

$$X=\langle x|x^{t}\rangle,\ Y=\langle y|y^{t}\rangle, C=\langle y|x^{t}\rangle \quad (1)$$

A linear estimate of the y-data from the x-data is (Eq. (2)):

$$y=Lx \quad (2)$$

where L is the optimal vector wiener filter solution that it is given by (Eq. (3)):

$$E=\langle (y-Lx)(y-Lx)^{t}\rangle \quad (3)$$

and E is minimized when $L = CX^{-1}$. Therefore, we have:

$$y=Lx=\left(CX^{-1}\right)x \quad (4)$$

and according to Eqs (3) and (4):

$$\varepsilon_{cc}=(y)-\left(\left(CX^{-1}\right)x\right) \quad (5)$$

where ε_{cc} is a change residual image. As depicted in the flowchart of the proposed method in Figure 1, Chronochrome is incorporated in the predictor phase on the hyperspectral data.

3.2 Z-score Analysis

The Z-Score provides the magnitude and directions of deviation from the mean of the distribution which is introduced in the distribution unit of standard deviation. The Z-score is defined in (Eq. (6)). as follows (Cheadle et al., 2002):

$$\text{modified-Z\_Score}=\sum_{i=1}^{N}\left((x_i-\text{mean}_i)/\text{std}_i\right) \quad (6)$$

In this study, a version of Z-Score value is adopted which is, in fact, a normalization that allows us to have the amplitude of change as the output of our proposed method. As stated in (Eq.(6)), the output of this procedure is a single band (Figure 4). The Z-Score analysis is then applied to the output of CC method in the analysis phase as depicted in the flowchart of a proposed method (Figure 1).

3.3 Otsu Algorithm

The Otsu algorithm is a group thresholding algorithm that performs image clustering automatically. The idea behind this approach is that the threshold value determines the weight of the variance within the minimum class value. The variance within the class is the variance of the total weight of each defined clusters(Ng, 2006; Otsu, 1979). In this study, the Otsu algorithm was applied for unsupervised preparation of training data for SVM classifier according as shown in the flowchart of the proposed method (Figure 1).

3.4 Endmember Extraction

The common method for producing 'multiple-change' information is classification, which was discussed in the introduction section. However, this paper proposes a new procedure for retrieving 'from-to' information without applying classification. In this regard, the proposed procedure uses estimation/extraction endmembers as well as the PCC algorithms. On the other hands, many methods are developed for estimating the number of endmembers. We apply the popular Harsanyi–Farrand–Chang (HFC) method which is based on the distribution of the differences of the eigenvalues of the correlation and the covariance matrices, respectively (Chang & Du, 2004). After estimating the number of endmembers, endmember extraction begins. Various endmember extraction methods exist in the literature including Simplex Identification via Split Augmented Lagrangian (SISAL)(Bioucas-Dias, 2009; Keshava & Mustard, 2002; Parente & Plaza, 2010). The SISAL algorithm is an unsupervised method for endmember extraction based on fitting a minimum volume simplex to the data subject to series of constraints. However, it is inevitable to estimate the number of endmembers before using SISAL algorithm(Bioucas-Dias, 2009). In this study, we apply the endmember extraction on the output of the CC algorithm as it can be observed in the flowchart of the proposed method (Figure 1).

3.5 Pearson Correlation Coefficient

The Pearson correlation coefficient (PCC) is one of the most popular measures for calculating the dependency between two spectral vectors. This measure is widely used in remote sensing applications(Wang, 2013). The PCC between spectral random vectors is defined as:

$$\text{PCC}=\frac{\text{cov}(x,y)}{\sigma_x\sigma_y} \quad (7)$$

where and x and y represent the target and reference spectra, and σ_x and σ_y are the standard deviations of x and y spectral vectors respectively. This study utilizes PCC in the decision phase for stacking layer data to retrieve the 'from-to'

information, as depicted in the flowchart of the proposed method (Figure 1).

3.6 Support Vector Machine

Support vector machine (SVM) is a supervised machine learning algorithm which is commonly used for classification purposes and is based on the statistical learning theory (Vapnik, 2013). SVM has recently been applied in classification of multispectral and hyperspectral remote sensing datasets successfully (George et al., 2014; Melgani & Bruzzone, 2004). The main idea behind SVM is to find a hyperplane that maximizes the margin between the two classes (Vladimir & Vapnik, 1995). This algorithm has several critical parameters including kernel parameters and the penalty coefficient (C). The popular kernels incorporated in SVM include polynomial, radial bias function, and linear kernels(Gaspar et al., 2012; Hasanlou et al., 2015). Different types of kernels and parameters for SVM are presented in Table 1.

This study incorporates SVM algorithm, in the decision phase, on the output of CC algorithm to make binary changes as illustrated in the flowchart of the proposed method (Figure 1).

4. Experiments

In this section, the experimental data and study area are discussed. Also, the results extracted from the proposed method evaluated by qualitative and quantitative criteria are presented. In addition, the change map results of the proposed method are compared with the most common and popular change detection algorithms.

4.1 Study Area

In this study, three different satellite (i.e. EO-1) hyperspectral image data sets are used for analyzing changes in wetlands and water bodies illustrated in (Figure 6) and (Table 2). The utilized two datasets to evaluate the performance of the proposed method. These datasets have been previously used in many hyperspectral change detection papers such as (S. Liu, 2015c; S. T. Seydi & Hasanlou, 2017; S. teymoor Seydi & Hasanlou, 2016b; Wu et al.,2012b) and they can be considered benchmark datasets. The ground truth datasets were developed by the authors through visual analysis and interpretation of the above-mentioned researches. Additionally, by using High-Resolution image datasets from Google Earth, a detailed visual comparison was carried out. Details and descriptions of each dataset will be presented in the next section. The Hyperion sensor contains 242 spectral bands with wavelengths between 0.4 and 2.5 micrometers and with a spatial resolution 30m and bandwidth of 7.5 km. Hyperion data were obtained at two separate range images using the push broom technology (Jafari & Lewis, 2012a). One of these spectra was a VNIR range which includes 70 bands between wavelength 356-1058 nm and SWIR wavelength consisting of 172 bands between wavelength 852-2577nm ("USGS EO-1," 2017).

4.1.1 Poyang Lake (dataset #1)

The Poyang lake located in Jiangxi Province is one of largest freshwater resource and biggest flood water storage wetland areas in China which is located within coordinates 28˚24′ to 29˚46′N, 115˚49′ to 116˚46′E (Chan & Xu, 2013; Yang & Yan, 2016). The extended area of the captured region in the hyperspectral dataset is 232×131 pixels. These datasets were acquired on 2004-July-16 and 2002-July-27 (Figure 6-a, b).

4.1.2 Umatilla River (dataset #2)

The Umatilla river is a gravel-bed river originating in the Blue Mountains of northeastern regions which flow into the Columbia River at Umatilla, OR, USA (Hughes, 2006). The extended area of the captured region in hyperspectral dataset contains 308×241 pixels and was acquired on 2004-May-01 and 2007-May-08 (Figure 6-c, d).

4.1.3 Shadegan Wetlands (dataset #3)

Shadegan wetland is one of the largest wetlands in Iran. This wetland is created by the downstream part of the river Jarahi and is located at coordinates 30°50´ to 31°00´N and

Table 1. Different type of kernels and parameters in the SVM classifier

Kernel type	Formula	Estimation parameters	Number parameters
Linear	$k(x,y)=x^T y$	C	1
Polynomial	$k(x,y)=(\gamma x^T y+\beta_0)^d$	d, γ, β_0, C	4
Radial basis function	$k(x,y)=e^{(-\gamma \|x-y\|^2)}$	γ , C	2

Table 2. The characteristic of datasets in different study areas

Datasets		Acquired date	# of bands	# of pixels	spatial resolution (m)	spectral resolution (nm)
Poyang Lake	#1	2002-July-27 2004-July-16	154	232×131	30	10
Umatilla River	#2	2004-May-01 2007-May-08	154	308×241	30	10
Shadegan Wetlands	#3	2006-June-06 2006-June-29	154	220×123	30	10

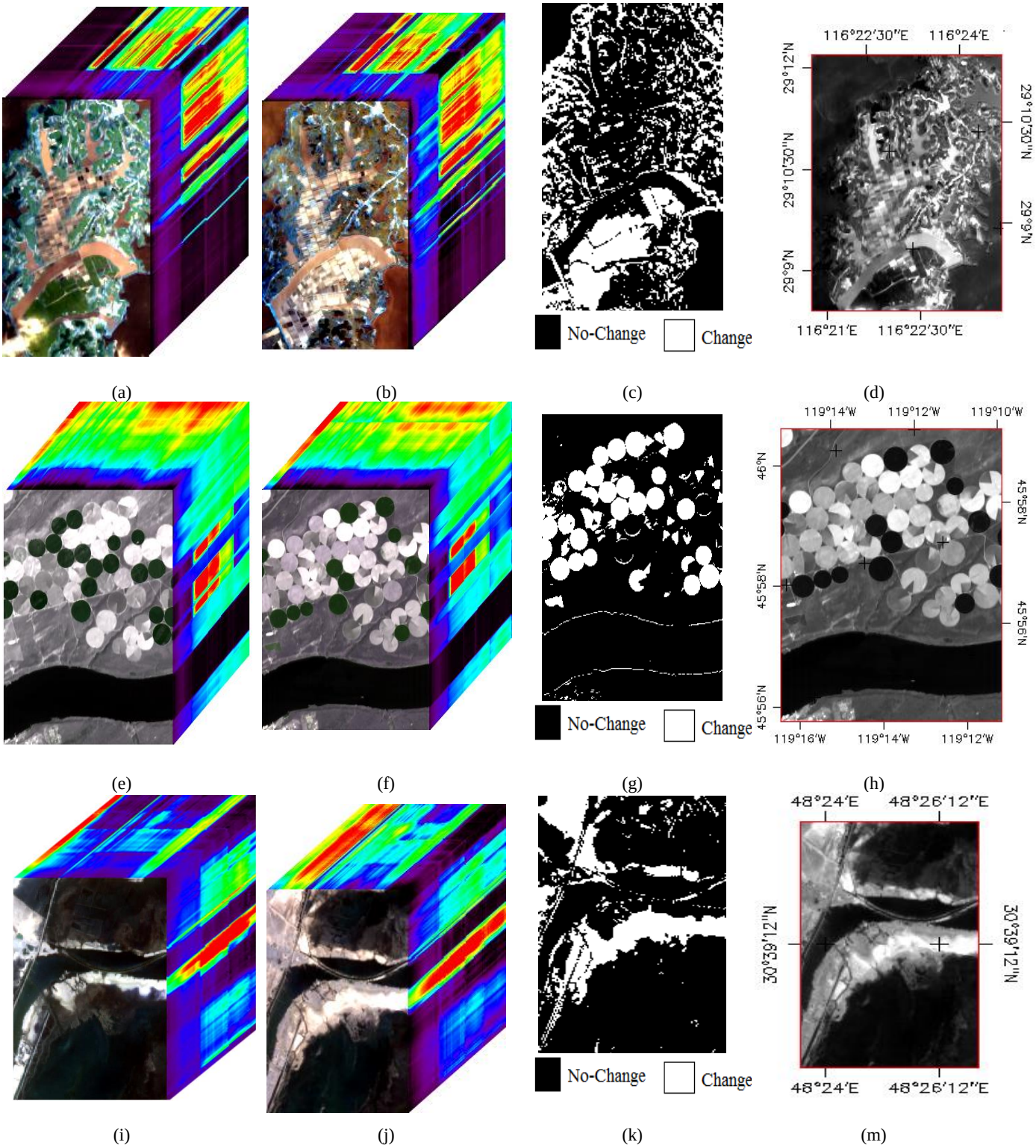

Figure 6. The (a) and (b) presented false color composite of the original hyperspectral images acquired in 2002 and 2004 of dataset #1 in China respectively, (c) ground truth, and (d) presented geographical location dataset #1. The (e) and (f) presented false color composite of the original hyperspectral images acquired in 2004 and 2007 of dataset #2 in USA respectively, (g) ground truth, and (h) presented geographical location dataset #2. The (i) and (j) present false color composite of the original hyperspectral images acquired in 2006 and 2006 of dataset #3 in Iran respectively, (k) ground truth, and (m) presented geographical location dataset #3

48°20´ to 49°20´E. The northern section of this wetland includes freshwater, and the salty water body is located in the southern part. Also, this wetland is home to different types of plants. The extent of the desired region extracted from EO-1 Hyperion satellite hyperspectral images was 220×123 pixels. In this area, we incorporate two multi-temporal data sets acquired on June 29th and June 6th of 2006. In Figure 6-e, f, a false-color composite of hyperspectral Shadegan wetland images for two different times is illustrated.

5. Implementation

Data pre-processing plays an important role before the

beginning of the main process and can be divided into two categories(Jafari & Lewis, 2012b): spectral and spatial correction. The pre-processing step starts with spectral correction processing; then spatial correction is applied. The first step of pre-processing consists of omitting no-data bands. In this regard, 44 bands (1-7, 58-76 and 225-242) were removed from our imagery (Jafari & Lewis, 2012a; Scheffler & Karrasch, 2013a). Also, of the 198 initial bands, two noisy bands including 77 and 78 as well as a number of other bands were removed (Datt et al., 2003; Khurshid et al., 2006). Therefore, 154 bands were selected in total as the input dataset for the proposed change detection method. In the second step, pixels in sample 129 and all lines are shifted to sample 256 in shortwave infrared (SWIR) spectral bands (Goodenough et al., 2003; Jafari & Lewis, 2012b). The third step is de-noising, de-striping, and also removing the zero-line by utilizing means and the global approach (Jafari & Lewis, 2012b; Scheffler & Karrasch, 2013b). The fourth pre-processing step is a radiometric correction. To achieve this goal, the digital number (DN) values of pixels are converted to physical radiance. The fifth step of the pre-processing is an atmospheric correction, which we used the FLAASH model. The final step of the pre-processing of the hyperspectral dataset is a spatial correction. The accuracy of the geometric correction (RMSE) was less of 0.4 pixel for all three datasets.

As already discussed, the outputs of the proposed method are (1) binary change map, (2) The amplitude of change map, and (3) the 'multiple-change' information map. The structure and details of the proposed method are illustrated in Figure 1. This work considered type of kernel which is widely utilized in the remote sensing community (Y. Liu & Parhi, 2016; Ring & Eskofier, 2016; Sakthivel et al., 2016; Shah-Hosseini et al., 2015c). To tune and select optimized SVM parameters (i.e. gamma ($\boldsymbol{\gamma}$) and penalty coefficient (C)), we performed a CV with GS procedures (Gu et al., 2017; Varma & Simon, 2006). Also, to have efficient kernel normalization, training and testing data were applied. In the normalization procedure, the data is mapped to values within the *[0,1]* span. The minimum and maximum values were selected based on minimum and maximum of training data. Table 3 presents the results obtained from tuning parameters for kernel and SVM (i.e. number of support vectors (# of SV), penalty coefficient (C) and gamma ($\boldsymbol{\gamma}$) parameter) for three data-sets. Addition, this table presented the optimum valves for SVM and kernels in two scenarios normalize and unnormalize.

Table 3. The results obtained from tuning SVM classifier and kernels parameters in different hyperspectral datasets

Datasets	**Normalize**	**Linear**		**Polynomial**					**Radial Bias Function**		
		C	# of SV	C	# of SV	γ	d	β_0	C	# of SV	γ
#1	Yes	2-8	210	2-3	16	2-7	3	1	2-6	17	2-7
	No	23	54	2-7	5	21: 220	3	1	2-3	48	2-7
#2	Yes	2-13	408	2-3	13	2-6	3	1	24	125	2-12
	No	25	206	2-6	6	20: 215	3	1	26	125	2-12
#3	Yes	29	5	2-6	608	2-9	3	1	23	65	2-3
	No	25	15	2-9	4	2-9: 29	3	1	25	61	2-5

Table 4. Performance of SVM classifier using type of kernels in different hyperspectral data-sets

Datasets		**#1**		**#2**		**#3**	
Kernel Function	Normalize	Overall Accuracy (%)	Kappa	Overall Accuracy (%)	Kappa	Overall Accuracy (%)	Kappa
Linear	Yes	96.77	0.927	97.16	0.907	92.73	0.756
	No	94.68	0.884	97.05	0.906	92.84	0.760
Polynomial	Yes	90.83	0.806	97.10	0.908	96.17	0.885
	No	88.11	0.705	94.75	0.816	89.57	0.628
Radial Bias Function	Yes	97.40	0.941	97.16	0.908	96.44	0.892
	No	96.65	0.922	9716	0.908	96.34	0.890

Table 5. The number of endmembers and false alarm probability (Pf) for different datasets

Datasets	**# of endmembers**	**P_f**
#1	6	10-3
#2	4	10-3
#3	3	10-5

The Table 4, presented a performance of SVM classifier using a type of kernels in different hyperspectral data-sets. The results show the RBF kernel has the best performance for three datasets. Also, the normalizing dataset improved the accuracy result of the CD. As mentioned in the above section, to have 'multiple-change' information in this study, we used HFC, SISAL and PCC algorithms. In the HFC algorithm, false alarm probability (P_f) parameter are assigned. A number of endmembers and false alarm probability is listed in Table 5. As we already discussed in previous sections, it is essential to compare and check the performance of the proposed method with common and popular CD methods. In this regard, we incorporated ground truth data for all three datasets to compute the validation criteria. In this paper, both quantitative and qualitative criteria were used for comparing the result. The popularly employed CD methods are principal component analysis (PCA) (Adar et al., 2011; Adar et al., 2014; K. M. Vongsy, 2007b), cross equalization (CE) (Adar et al., 2011; Michael et al.,2008b; Michael et al.,2012), spectral angle mapper (SAM) (Adar et al., 2011), subspace based (SSB) (Wu et al., 2013), multivariate alternative detection (MAD) (Nielsena & Müllerb, 2003b), and iterative reweight-MAD (IR-MAD) (Nielsen, 2007; S. teymoor Seydi & Hasanlou, 2016b). All of these methods require assigning suitable thresholds. In this study, unsupervised segmentation by incorporating Otsu algorithm was used to set these thresholds.

Therefore, by considering the optimum kernel parameters (Tables 3) for SVM classification for all datasets (#1, #2 and #3) the proposed method begins. Figure 7 shows a visual analysis of the proposed method and other CD methods on multi-temporal hyperspectral datasets #1. As it is clear in Figure 7, the proposed method can detect all changes and provide information about the features changes including the 'multiple-change' change map as well as the amplitude of changes in the map. This observation empirically proves that the proposed method nearly detects all of the change compared to the other techniques. In the endmember extraction section, we described that the SISAL and HFC methods were used to obtain the 'multiple-change' map. Hence, six classes detected and produced the 'multiple-change' change map (Figure 7-c) for dataset #1. The Figure 7-b shows the amplitude of changes where the changing intensity is clearly highlighted.

The Same computational approach is applied on dataset #2. Figure 8 shows changes of Umatilla River where there are many land cover change types in areas that contain different agricultural fields. Also, in this figure, there are low changes in the edges of the river. In this dataset (#2), 'multiple-change' change map has four classes which are detected by proposed method (Figure 8-c).

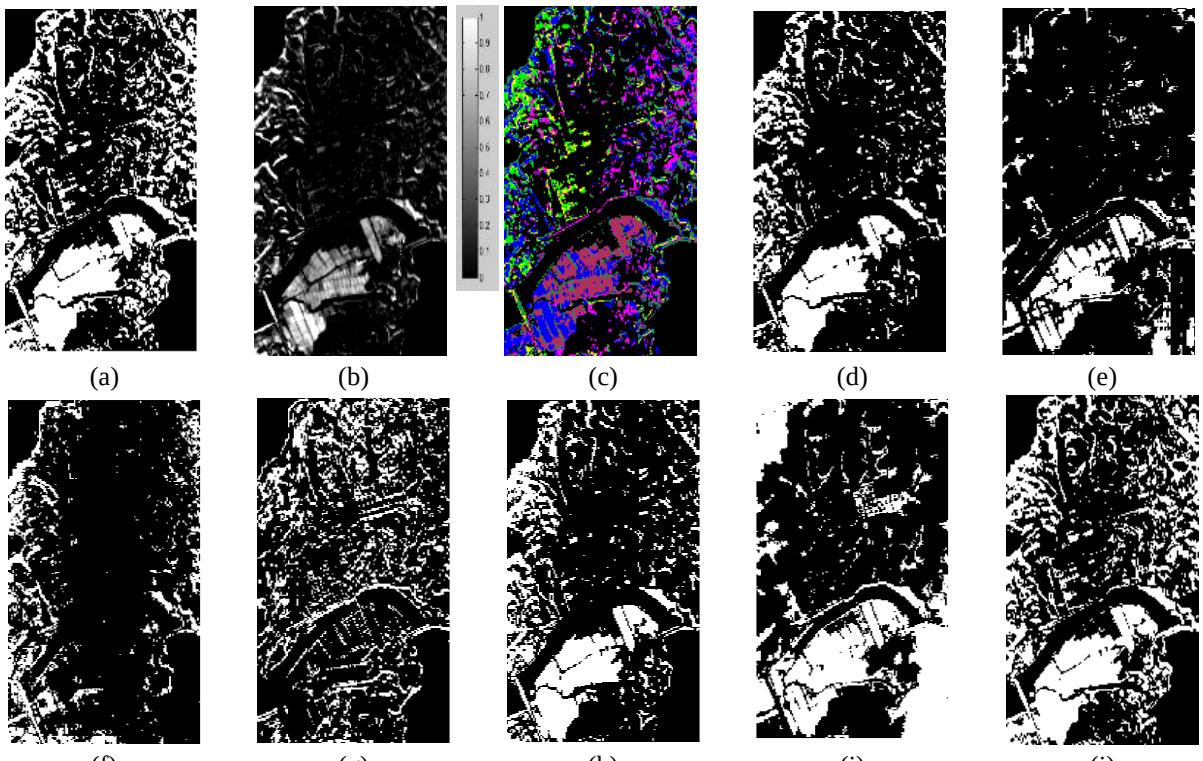

Figure 7. The results of CD methods for dataset #1. (a) Proposed method-binary change map, (b) Proposed method-amplitude of change map, (c) Proposed method-'from-to' map, (d) CE, (e) SSB, (f) IR-MAD, (g) MAD, (h) PCA, (i) SAM, and (j) Ground truth

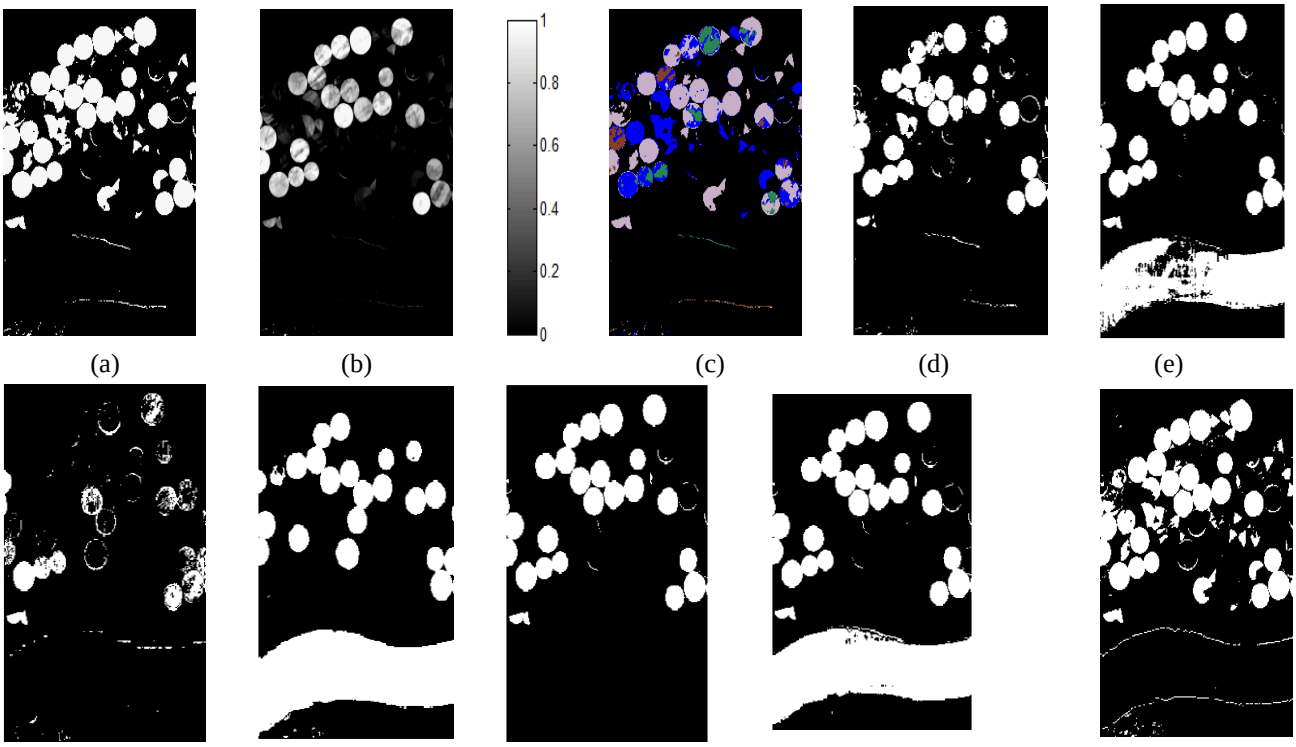

Figure 8. The results of CD methods for dataset #2. (a) Proposed method-binary change map, (b) Proposed method-amplitude of change map, (c) Proposed method-'from-to' map, (d) CE, (e) SSB, (f) IR-MAD, (g) MAD, (h) PCA, (i) SAM, and (j) Ground truth

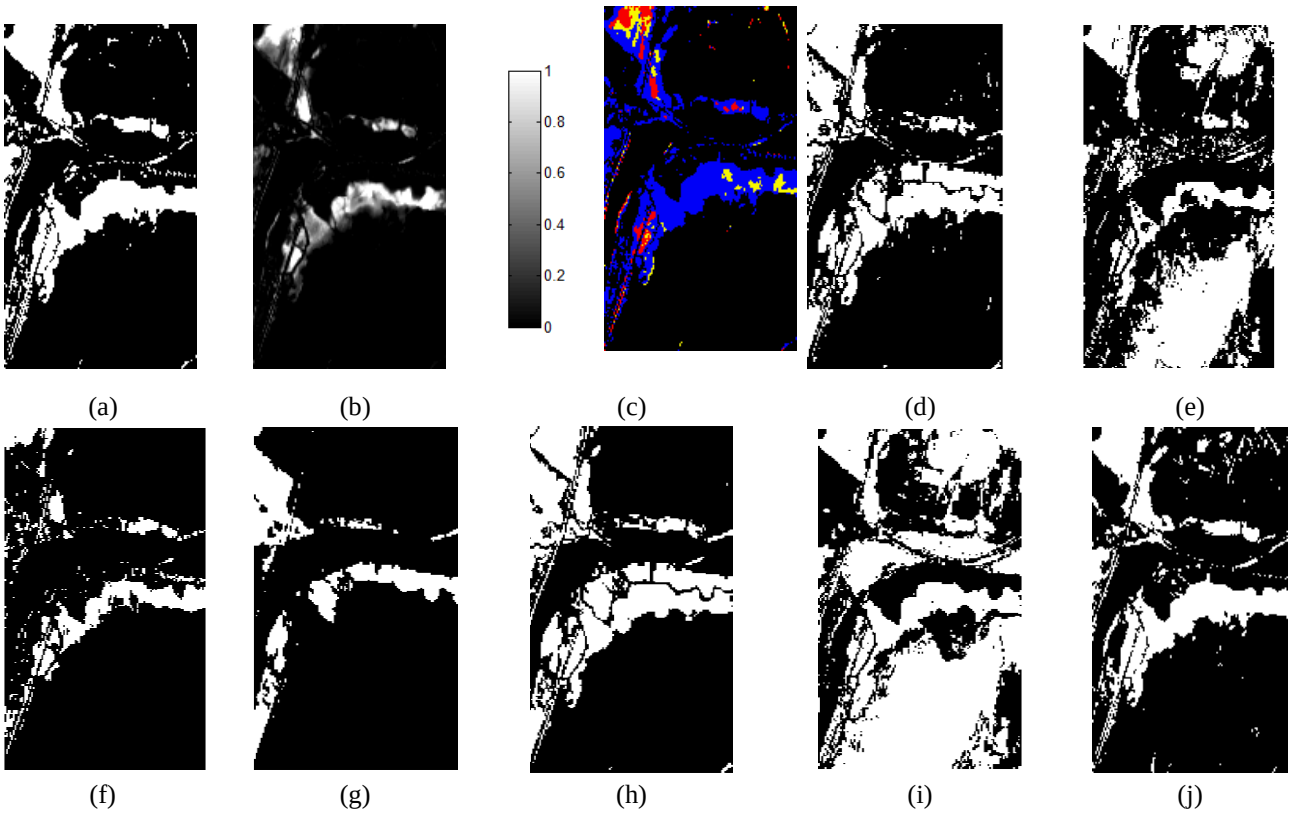

Figure 9. The results of CD methods for dataset #3. (a) Proposed method-binary change map, (b) Proposed method-amplitude of change map, (c) Proposed method-'from-to' map, (d) CE, (e) SSB, (f) IR-MAD, (g) MAD, (h) PCA, (i) SAM, and (j) Ground truth

Table 6. Performance of proposed method and other common CD methods for all hyperspectral datasets

Datasets	Indices	SAM	IR-MAD	MAD	CE	SBB	PCA	Proposed Method
#1	Overall	66.01	67.07	65.76	88.89	73.11	89.58	97.40
	Kappa	0.223	0.038	0.143	0.727	0.299	0.747	0.941
#2	Overall	75.53	83.85	67.51	93.70	77.855	93.24	97.16
	Kappa	0.371	0.304	0.159	0.778	0.400	0.756	0.907
#3	Overall	52.42	86.06	69.53	83.44	63.86	81.81	96.42
	Kappa	0.111	0.498	0.092	0.527	0.144	0.485	0.890

In Figure 8, some algorithms show a certain level of sensitivity to the waterbody area such as the results presented in Figure 8-g, e, f. On the other hands, one can clearly observe from the results (Figure 8-a, b, c) that the proposed method has excellent performance compared to other approaches in this area.

Similarly, Figure 9 presents the results of the CD methods on Shadegan wetland (data-set #3). In this region, the main changes are originated from seasonal changes in the water level. The proposed method can find three different classes for change area (Figure 9-c). As it is clear from the Figures, the similarity-based methods such as SAM technique are not suitable for monitoring the changes due to the extraction of a false alarm pixels.

After the primary observational analysis, we perform the numerical evaluation. In this regard, two common measures are used for evaluating performance and accuracy of CD methods which include overall accuracy, and kappa coefficient. All implemented CD methods are supervised and their related accuracy is usually computed by examining the best threshold value selection. That means each threshold has a correlation with the accuracy, and maximum accuracy is considered as the final accuracy. Table 6 presents the accuracy of the proposed method for RBF kernel and other CD techniques. We can clearly observe the superiority of the proposed method compared to other methods in all three different hyperspectral datasets in Table 5. Also, as presented in Table 5, the PCA and CE methods have efficiencies close to the proposed method, especially for hyperspectral dataset #1 and hyperspectral dataset #2. The IR-MAD algorithm has good performance compare to MAD algorithm. The SAM and SSB have low performance due to sensitive to noise and atmospheric conditions. These methods utilizing continuous spectral signatures nevertheless, this issue caused to don't suitable for wetland and waterbody change detection using hyperspectral imagery. This paper proposed a new change detection method on hyperspectral imagery which included observational and numerical analysis and comparison with other common HCD methods. The proposed method provides three different outputs which provide more detail about the changes, and thus helps understanding changes while the other CD methods do not give three outputs together. The lecture review in introduction section, the type of change detection methods in 5 main groups considered. The challenges and advantages discussed, the results of CD certified this issues of CD methods. Addition, more details of visual and numerical analysis show that: (1) the hyperspectral imagery has a high capability for CD in waterbodies and wetlands, (2) the CE methods provides better results among common HCD methods, (3) some techniques, such as SSB and SAM, are not suitable for water-body change detection due to their high sensitivity, (4) the proposed method has the highest accuracy for all employed datasets, therefore it is efficient for water-body area, and (5) finally, the proposed methods provide more detail of changes that can help improve the decision making process.

6. Conclusion

Wetlands are critical ecosystems where changes occur frequently and widely. Therefore, creating a framework for monitoring the changes in these ecosystems is essential. In this regards, studying methods that are able to perform accurate change detection in these areas is crucial. This paper presents a new hybrid method for achieving precise and informative change maps using hyperspectral imagery without requiring prior knowledge of the wetlands and water-body area. We first discussed all the issues related to CDs using hyperspectral imagery. Therefore, a new change detection method was proposed to address these issues. The proposed hybrid method uses four groups of CD methods to enhance the content and quality of final CD results. The experiments were applied on three real hyperspectral datasets on wetland and waterbody areas from different regions and countries. The output results showed: (1) the hyperspectral imagery has high potential to monitoring and assessment of wetland and waterbody areas, however, for this purpose need to special techniques; (2) the visual and numerical analysis proved the excellent performance proposed method for hyperspectral change detection compare to other methods; (3) superiority of the proposed unsupervised method without requiring prior knowledge of changes while some CD methods need to training data or setting parameters; (4) the fact that this method can provide binary change map as well as the information about change structure ('multiple-change' map) and also the amplitude map; (5) the use of normalize data and RBF kernel improved the accuracy CD, significantly, and (6) the fact that the implementation of the proposed method is simple and has high efficiency in comparison to other famous and commonly used CD methods like (PCA, CE, IR-MAD, SSB, SAM).

References

Adar, S., Notesco, G., Brook, A., Livne, I., Rojik, P., Kopackova, V., ... & Ehrler, C. (2011, October). Change detection over Sokolov open-pit mining area, Czech Republic, using multi-temporal HyMAP data (2009-2010). In *Image and Signal Processing for Remote Sensing XVII* (Vol. 8180, p. 81800T). International Society for Optics and Photonics.

Adar, S., Shkolnisky, Y., & Dor, E. B. (2012, July). New approach for spectral change detection assessment using multistrip airborne hyperspectral data. In *Geoscience and Remote Sensing Symposium (IGARSS), 2012 IEEE International* (pp. 4966-4969). IEEE.

Ahlqvist, O. (2008). Extending post-classification change detection using semantic similarity metrics to overcome class heterogeneity: A study of 1992 and 2001 US National Land Cover Database changes. *Remote Sensing of Environment*, *112*(3), 1226-1241.

Barrett, E. C. (2013). *Introduction to environmental remote sensing*. Routledge.

Bioucas-Dias, J. M. (2009, August). A variable splitting augmented Lagrangian approach to linear spectral unmixing. In *Hyperspectral Image and Signal Processing: Evolution in Remote Sensing, 2009. WHISPERS'09. First Workshop on* (pp. 1-4). IEEE.

Bovolo, F., & Bruzzone, L. (2015). The time variable in data fusion: A change detection perspective. *IEEE Geoscience and Remote Sensing Magazine*, *3*(3), 8-26.

Bovolo, F., Marchesi, S., & Bruzzone, L. (2012). A framework for automatic and unsupervised detection of multiple changes in multitemporal images. *IEEE Transactions on Geoscience and Remote Sensing*, *50*(6), 2196-2212.

Castellana, L., D'Addabbo, A., & Pasquariello, G. (2007). A composed supervised/unsupervised approach to improve change detection from remote sensing. *Pattern Recognition Letters*, *28*(4), 405-413.

Chang, C. I., & Du, Q. (2004). Estimation of number of spectrally distinct signal sources in hyperspectral imagery. *IEEE Transactions on geoscience and remote sensing*, *42*(3), 608-619.

Chan, K. K. Y., & Xu, B. (2013). Perspective on remote sensing change detection of Poyang Lake wetland. *Annals of GIS*, *19*(4), 231-243.

Cheadle, C., Cho-Chung, Y. S., Becker, K. G., & Vawter, M. P. (2003). Application of z-score transformation to Affymetrix data. *Applied bioinformatics*, *2*(4), 209-217.

Datt, B., McVicar, T. R., Van Niel, T. G., Jupp, D. L., & Pearlman, J. S. (2003). Preprocessing EO-1 Hyperion hyperspectral data to support the application of agricultural indexes. *IEEE Transactions on Geoscience and Remote Sensing*, *41*(6), 1246-1259.

Dronova, I., Gong, P., & Wang, L. (2011). Object-based analysis and change detection of major wetland cover types and their classification uncertainty during the low water period at Poyang Lake, China. *Remote Sensing of Environment*, *115*(12), 3220-3236.

Eismann, M. T., Meola, J., & Hardie, R. C. (2008). Hyperspectral change detection in the presenceof diurnal and seasonal variations. *IEEE Transactions on Geoscience and Remote Sensing*, *46*(1), 237-249.

Franklin, S. E., Ahmed, O. S., Wulder, M. A., White, J. C., Hermosilla, T., & Coops, N. C. (2015). Large area mapping of annual land cover dynamics using multitemporal change detection and classification of Landsat time series data. *Canadian Journal of Remote Sensing*, *41*(4), 293-314.

Fröjse, L. (2011). Multitemporal satellite images for urban change detection.

Gaspar, P., Carbonell, J., & Oliveira, J. L. (2012). On the parameter optimization of Support Vector Machines for binary classification. *Journal of integrative bioinformatics*, *9*(3), 33-43.

George, R., Padalia, H., & Kushwaha, S. P. S. (2014). Forest tree species discrimination in western Himalaya using EO-1 Hyperion. *International Journal of Applied Earth Observation and Geoinformation*, *28*, 140–149.

Ghobadi, Y., Pradhan, B., Shafri, H. Z., bin Ahmad, N., & Kabiri, K. (2015). Spatio-temporal remotely sensed data for analysis of the shrinkage and shifting in the Al Hawizeh wetland. *Environmental Monitoring and Assessment*, *187*(1), 1–17. https://doi.org/10.1007/s10661-014-4156-0

Gibbes, C., Southworth, J., & Keys, E. (2009). Wetland conservation: change and fragmentation in Trinidad's protected areas. *Geoforum*, *40*(1), 91–104.

Gómez, C., White, J. C., & Wulder, M. A. (2016). Optical remotely sensed time series data for land cover classification: A review. *ISPRS Journal of Photogrammetry and Remote Sensing*, *116*, 55–72.

Goodenough, D. G., Dyk, A., Niemann, K. O., Pearlman, J. S., Chen, H., Han, T., … West, C. (2003). Processing Hyperion and ALI for forest classification. *IEEE Transactions on Geoscience and Remote Sensing*, *41*(6), 1321–1331. https://doi.org/10.1109/TGRS.2003.813214

Gu, B., Sheng, V. S., Tay, K. Y., Romano, W., & Li, S. (2017). Cross Validation Through Two-Dimensional Solution Surface for Cost-Sensitive SVM. *IEEE Transactions on Pattern Analysis and Machine Intelligence*, *39*(6), 1103–1121.

Gunawardena, A., Fernando, T., Takeuchi, W., Wickramasinghe, C. H., & Samarakoon, L. (2014). Identification, evaluation and change detection of highly sensitive wetlands in South-Eastern Sri Lanka using ALOS (AVNIR2, PALSAR) and Landsat ETM+ data. In *IOP Conference Series: Earth and Environmental Science* (Vol. 20, p. 012050). IOP Publishing.

Hasanlou, M., Samadzadegan, F., & Homayouni, S. (2015).

SVM-based hyperspectral image classification using intrinsic dimension. *Arabian Journal of Geosciences*, *8*(1), 477–487.

Hasanlou, M., & Seydi, S. T. (2018). Hyperspectral Change Detection: An Experimental Comparative Study. *International Journal of Remote Sensing*, 1-45.

Hegazy, I. R., & Kaloop, M. R. (2015). Monitoring urban growth and land use change detection with GIS and remote sensing techniques in Daqahlia governorate Egypt. *International Journal of Sustainable Built Environment*, *4*(1), 117–124.

Huang, S., Ramirez, C., Kennedy, K., Mallory, J., Wang, J., & Chu, C. (2017). Updating land cover automatically based on change detection using satellite images: case study of national forests in Southern California. *GIScience & Remote Sensing*, 1–20.

Hughes, M. L., McDowell, P. F., & Marcus, W. A. (2006). Accuracy assessment of georectified aerial photographs: implications for measuring lateral channel movement in a GIS. *Geomorphology*, *74*(1–4), 1–16.

Hussain, M., Chen, D., Cheng, A., Wei, H., & Stanley, D. (2013). Change detection from remotely sensed images: From pixel-based to object-based approaches. *ISPRS Journal of Photogrammetry and Remote Sensing*, *80*, 91–106.

Jafari, R., & Lewis, M. M. (2012). Arid land characterisation with EO-1 Hyperion hyperspectral data. *International Journal of Applied Earth Observation and Geoinformation*, *19*, 298–307.

Jiang, F., Qi, S., Liao, F., Ding, M., & Wang, Y. (2014). Vulnerability of Siberian crane habitat to water level in Poyang Lake wetland, China. *GIScience & Remote Sensing*, *51*(6), 662–676.

Kayastha, N., Thomas, V., Galbraith, J., & Banskota, A. (2012). Monitoring wetland change using inter-annual landsat time-series data. *Wetlands*, *32*(6), 1149–1162.

Keramitsoglou, I., Stratoulias, D., Fitoka, E., Kontoes, C., & Sifakis, N. (2015). A transferability study of the kernel-based reclassification algorithm for habitat delineation. *International Journal of Applied Earth Observation and Geoinformation*, *37*, 38–47.

Keshava, N. (2003). A survey of spectral unmixing algorithms. *Lincoln laboratory journal*, *14*(1), 55–78.

Khurshid, K. S., Staenz, K., Sun, L., Neville, R., White, H. P., Bannari, A., Champagne, C. M., et al. (2006). Preprocessing of EO-1 Hyperion data. *Canadian Journal of Remote Sensing*, *32*(2), 84–97.

Kumar, L., & Sinha, P. (2014). Mapping salt-marsh land-cover vegetation using high-spatial and hyperspectral satellite data to assist wetland inventory. *GIScience & Remote Sensing*, *51*(5), 483–497.

Lee, S. (2011). Detecting Wetland Change through Supervised Classification of Landsat Satellite Imagery within the Tunkwa Watershed of British Columbia, Canada. Retrieved January 10, 2017, from http://www.diva-portal.org/smash/record.jsf?pid=diva2:681571

Li, H., Zhang, D., Zhang, Y., & Xu, Y. (2008). Research of image preprocessing methods for EO-1 Hyperion hyperspectral data in tidal flat area. *Geoinformatics*, 71471G–71471G.

Liu, S. (2015). *Advanced Techniques for Automatic Change Detection in Multitemporal Hyperspectral Images*. University of Trento. Retrieved January 10, 2017, from http://eprints-phd.biblio.unitn.it/1393/

Liu, Y., & Parhi, K. K. (2016). Computing RBF kernel for SVM classification using stochastic logic. *Signal Processing Systems (SiPS), 2016 IEEE International Workshop on* (pp. 327–332). IEEE.

Lu, D., Moran, E., Hetrick, S., & Li, G. (2011). Land-use and land-cover change detection. *Advances in Environmental Remote Sensing Sensors, Algorithms, and Applications. CRC Press Taylor & Francis Group, New York*, 273–290.

Mabwoga, S. O., & Thukral, A. K. (2014). Characterization of change in the Harike wetland, a Ramsar site in India, using landsat satellite data. *SpringerPlus*, *3*(1), 576.

McCarthy, M. J., Merton, E. J., & Muller-Karger, F. E. (2015). Improved coastal wetland mapping using very-high 2-meter spatial resolution imagery. *International Journal of Applied Earth Observation and Geoinformation*, *40*, 11–18.

Melgani, F., & Bruzzone, L. (2004). Classification of hyperspectral remote sensing images with support vector machines. *IEEE Transactions on geoscience and remote sensing*, *42*(8), 1778–1790.

Mereta, S. T., Boets, P., Bayih, A. A., Malu, A., Ephrem, Z., Sisay, A., Endale, H., et al. (2012). Analysis of environmental factors determining the abundance and diversity of macroinvertebrate taxa in natural wetlands of Southwest Ethiopia. *Ecological Informatics*, *7*(1), 52–61.

Mousazadeh, R., Ghaffarzadeh, H., Nouri, J., Gharagozlou, A., & Farahpour, M. (2015). Land use change detection and impact assessment in Anzali international coastal wetland using multi-temporal satellite images. *Environmental monitoring and assessment*, *187*(12), 1–11.

Ng, H.-F. (2006). Automatic thresholding for defect detection. *Pattern recognition letters*, *27*(14), 1644–1649.

Nielsen, A. A. (2007). The regularized iteratively reweighted MAD method for change detection in multi-and hyperspectral data. *IEEE Transactions on Image processing*, *16*(2), 463–478.

Nielsena, A. A., & Müllerb, A. (2003). Change detection by the MAD method in hyperspectral image data. Retrieved May 9, 2017, from http://citeseerx.ist.psu.edu/viewdoc/summary?

doi=10.1.1.608.8367

Omo-Irabor, O. O. (2016). A Comparative Study of Image Classification Algorithms for Landscape Assessment of the Niger Delta Region. *Journal of Geographic Information System*, *8*(02), 163.

Otsu, N. (1979). A threshold selection method from gray-level histograms. *IEEE transactions on systems, man, and cybernetics*, *9*(1), 62–66.

Pacifici, F. (2007). Change detection algorithms: State of the art. *URL: http://www. disp. uniroma2. it/earth_observatio n/pdf/CD-Algorithms. pdf (Accessed on 4 November, 2011)*.

Parente, M., & Plaza, A. (2010). Survey of geometric and statistical unmixing algorithms for hyperspectral images. *Hyperspectral Image and Signal Processing: Evolution in Remote Sensing (WHISPERS), 2010 2nd Workshop on* (pp. 1–4). IEEE.

Pieper, M., Manolakis, D., Cooley, T., Brueggeman, M., Weisner, A., & Jacobson, J. (2015). New insights and practical considerations in hyperspectral change detection. *2015 IEEE International Geoscience and Remote Sensing Symposium (IGARSS)* (pp. 4161–4164). IEEE.

Rapinel, S., Hubert-Moy, L., & Clément, B. (2015). Combined use of LiDAR data and multispectral earth observation imagery for wetland habitat mapping. *International journal of applied earth observation and geoinformation*, *37*, 56–64.

Ring, M., & Eskofier, B. M. (2016). An approximation of the Gaussian RBF kernel for efficient classification with SVMs. *Pattern Recognition Letters*, *84*, 107–113.

Romshoo, S. A., & Rashid, I. (2014). Assessing the impacts of changing land cover and climate on Hokersar wetland in Indian Himalayas. *Arabian Journal of Geosciences*, *7*(1), 143–160.

Sakthivel, N. R., Saravanamurugan, S., Nair, B. B., Elangovan, M., & Sugumaran, V. (2016). Effect of kernel function in support vector machine for the fault diagnosis of pump. *Journal of Engineering Science and Technology*, *11*(6), 826–838.

Samadzadegan, F., Hasani, H., & Schenk, T. (2012). Simultaneous feature selection and SVM parameter determination in classification of hyperspectral imagery using ant colony optimization. *Canadian Journal of Remote Sensing*, *38*(2), 139–156.

Schaum, A., & Stocker, A. (1998). Long-interval chronochrome target detection. *Proc. 1997 International Symposium on Spectral Sensing Research* (pp. 1760–1770).

Scheffler, D., & Karrasch, P. (2013). Preprocessing of hyperspectral images: a comparative study of destriping algorithms for EO1-hyperion. *Image and Signal Processing for Remote Sensing XIX* (Vol. 8892, p. 88920H). International Society for Optics and Photonics.

Seydi, S. T., & Hasanlou, M. (2017). A new land-cover match-based change detection for hyperspectral imagery. *European Journal of Remote Sensing*, *50*(1), 517–533.

Seydi, S. T., & Hasanlou, M. (2018). Sensitivity analysis of pansharpening in hyperspectral change detection. *Applied Geomatics*, 1–11.

Seydi, S. teymoor, & Hasanlou, M. (2016). Novel Wetland and Water Body Change Detction using Multitemporal Hyperspectral Imagery. Presented at the International Water Conference 2016 on Water Resources in Arid Areas, Oman,Muscat: Springer.

Shah-Hosseini, R., Homayouni, S., & Safari, A. (2015). A hybrid kernel-based change detection method for remotely sensed data in a similarity space. *Remote Sensing*, *7*(10), 12829–12858.

Sica, Y. V., Quintana, R. D., Radeloff, V. C., & Gavier-Pizarro, G. I. (2016). Wetland loss due to land use change in the Lower Paraná River Delta, Argentina. *Science of the Total Environment*, *568*, 967–978.

Singh, A. (1989). Review article digital change detection techniques using remotely-sensed data. *International journal of remote sensing*, *10*(6), 989–1003.

Smith, R. (2012). Introduction to Hyperspectral Imaging, MicroImages Inc. *Mentor, OH*. Retrieved from http://www.microimages.com/documentation/Tutorials/hyprspec.pdf

Storey, E. A., Stow, D. A., Coulter, L. L., & Chen, C. (2017). Detecting shadows in multi-temporal aerial imagery to support near-real-time change detection. *GIScience & Remote Sensing*, 1–18.

Taminskasa, J., Petro\liusa, R., \Limanauskienėa, R., Satkūnasb, J., & Linkevičienėa, R. (2013). Prediction of change in wetland habitats by groundwater: case study in Northeast Lithuania. *Estonian Journal of Earth Sciences*, *62*(2), 57ø e72.

Thonfeld, F., Feilhauer, H., Braun, M., & Menz, G. (2016). Robust Change Vector Analysis (RCVA) for multi-sensor very high resolution optical satellite data. *International Journal of Applied Earth Observation and Geoinformation*, *50*, 131–140.

Varma, S., & Simon, R. (2006). Bias in error estimation when using cross-validation for model selection. *BMC bioinformatics*, *7*(1), 91.

Vladimir, V. N., & Vapnik, V. (1995). *The nature of statistical learning theory*. Springer Heidelberg.

Vongsy, K. M. (2007). *Change detection methods for hyperspectral imagery*. Wright State University. Retrieved January 10, 2017, from https://etd.ohiolink.edu/!etd.send_file?accession=wright1184010751&disposition=attachment

Vongsy, K., Mendenhall, M. J., Hanna, P. M., & Kaufman, J. (2009). Change detection using synthetic hyperspectral imagery. *Hyperspectral Image and Signal Processing: Evolution in Remote Sensing, 2009. WHISPERS'09. First*

Workshop on (pp. 1–4). IEEE. Retrieved May 21, 2017, from http://ieeexplore.ieee.org/abstract/document/5289016/

Wang, J. (2013). Pearson correlation coefficient. *Encyclopedia of Systems Biology* (pp. 1671–1671). Springer. Retrieved January 28, 2017, from http://link.springer.com/content/pdf/10.1007/978-1-4419-9863-7_372.pdf

White, L., Brisco, B., Dabboor, M., Schmitt, A., & Pratt, A. (2015). A collection of SAR methodologies for monitoring wetlands. *Remote sensing*, *7*(6), 7615–7645.

Whiteside, T. G., & Bartolo, R. E. (2015). Use of WorldView-2 time series to establish a wetland monitoring program for potential offsite impacts of mine site rehabilitation. *International Journal of Applied Earth Observation and Geoinformation*, *42*, 24–37.

Wu, C., Du, B., & Zhang, L. (2013). A subspace-based change detection method for hyperspectral images. *IEEE Journal of selected topics in applied earth observations and remote sensing*, *6*(2), 815–830.

Wu, C., Zhang, L., & Du, B. (2012). Targeted change detection for stacked multi-temporal hyperspectral image. *Hyperspectral Image and Signal Processing (WHISPERS), 2012 4th Workshop on* (pp. 1–4). IEEE. Retrieved July 31, 2017, from http://ieeexplore.ieee.org/abstract/document/6874282/

Yang, Y., & Yan, Z. (2016). Monitoring and Analyzing of Poyang Lake Wetland Land Use Change Based on RS and GIS. *Geo-Informatics in Resource Management and Sustainable Ecosystem* (pp. 213–221). Springer.

Yuan, F., Sawaya, K. E., Loeffelholz, B. C., & Bauer, M. E. (2005). Land cover classification and change analysis of the Twin Cities (Minnesota) Metropolitan Area by multitemporal Landsat remote sensing. *Remote sensing of Environment*, *98*(2), 317–328.

Yuen, P. W., & Richardson, M. (2010). An introduction to hyperspectral imaging and its application for security, surveillance and target acquisition. *The Imaging Science Journal*, *58*(5), 241–253.

Zanotta, D. C., Zani, H., & Shimabukuro, Y. E. (2013). Automatic detection of burned areas in wetlands by remote sensing multitemporal images. *Geoscience and Remote Sensing Symposium (IGARSS), 2013 IEEE International* (pp. 1959–1962). IEEE.

Zhao, H., Cui, B., Zhang, H., Fan, X., Zhang, Z., & Lei, X. (2010). A landscape approach for wetland change detection (1979-2009) in the Pearl River Estuary. *Procedia Environmental Sciences*, *2*, 1265–1278.

chmitt, A., & Pratt, A. (2015). A collection of SAR methodologies for monitoring wetlands. *Remote sensing*, *7*(6), 7615–7645.

Whiteside, T. G., & Bartolo, R. E. (2015). Use of WorldView-2 time series to establish a wetland monitoring program for potential offsite impacts of mine site rehabilitation. *International Journal of Applied Earth Observation and Geoinformation*, *42*, 24–37.

Wu, C., Du, B., & Zhang, L. (2013). A subspace-based change detection method for hyperspectral images. *IEEE Journal of selected topics in applied earth observations and remote sensing*, *6*(2), 815–830.

Wu, C., Zhang, L., & Du, B. (2012). Targeted change detection for stacked multi-temporal hyperspectral image. *Hyperspectral Image and Signal Processing (WHISPERS), 2012 4th Workshop on* (pp. 1–4). IEEE. Retrieved July 31, 2017, from http://ieeexplore.ieee.org/abstract/document/6874282/

Yang, Y., & Yan, Z. (2016). Monitoring and Analyzing of Poyang Lake Wetland Land Use Change Based on RS and GIS. *Geo-Informatics in Resource Management and Sustainable Ecosystem* (pp. 213–221). Springer.

Yuan, F., Sawaya, K. E., Loeffelholz, B. C., & Bauer, M. E. (2005). Land cover classification and change analysis of the Twin Cities (Minnesota) Metropolitan Area by multitemporal Landsat remote sensing. *Remote sensing of Environment*, *98*(2), 317–328.

Yuen, P. W., & Richardson, M. (2010). An introduction to hyperspectral imaging and its application for security, surveillance and target acquisition. *The Imaging Science Journal*, *58*(5), 241–253.

Zanotta, D. C., Zani, H., & Shimabukuro, Y. E. (2013). Automatic detection of burned areas in wetlands by remote sensing multitemporal images. *Geoscience and Remote Sensing Symposium (IGARSS), 2013 IEEE International* (pp. 1959–1962). IEEE.

Zhao, H., Cui, B., Zhang, H., Fan, X., Zhang, Z., & Lei, X. (2010). A landscape approach for wetland change detection (1979-2009) in the Pearl River Estuary. *Procedia Environmental Sciences*, *2*, 1265–1278.